Constitutive activation of a plasma membrane H^+-ATPase prevents abscisic acid-mediated stomatal closure

Sylvain Merlot[1], Nathalie Leonhardt[2,5], Francesca Fenzi[1,5], Christiane Valon[1], Miguel Costa[2,4], Laurie Piette[2], Alain Vavasseur[2], Bernard Genty[2], Karine Boivin[1], Axel Müller[3], Jérôme Giraudat[1] and Jeffrey Leung[1,*]

[1]Institut des Sciences du Végétal, Centre National de la Recherche Scientifique, UPR 2355, Gif-sur-Yvette, France, [2]CEA Cadarache, DSV, UMR 6191 CEA-CNRS, DEVM, LEMS and LEMP, St Paul les Durance Cedex, France and [3]CarboGen AG, Aarau, Switzerland

Light activates proton (H^+)-ATPases in guard cells, to drive hyperpolarization of the plasma membrane to initiate stomatal opening, allowing diffusion of ambient CO_2 to photosynthetic tissues. Light to darkness transition, high CO_2 levels and the stress hormone abscisic acid (ABA) promote stomatal closing. The overall H^+-ATPase activity is diminished by ABA treatments, but the significance of this phenomenon in relationship to stomatal closure is still debated. We report two dominant mutations in the *OPEN STOMATA2* (*OST2*) locus of *Arabidopsis* that completely abolish stomatal response to ABA, but importantly, to a much lesser extent the responses to CO_2 and darkness. The *OST2* gene encodes the major plasma membrane H^+-ATPase AHA1, and both mutations cause constitutive activity of this pump, leading to necrotic lesions. H^+-ATPases have been traditionally assumed to be general endpoints of all signaling pathways affecting membrane polarization and transport. Our results provide evidence that AHA1 is a distinct component of an ABA-directed signaling pathway, and that dynamic downregulation of this pump during drought is an essential step in membrane depolarization to initiate stomatal closure.

Introduction

Plasma membrane proton (H^+)-ATPases in protozoa, fungi and plants create proton gradients that activate many

*Corresponding author. CNRS Science de la Vie, Institut des Sciences du Végétal, UPR 2355, 1 Avenue de la Terrasse Bat. 23, Gif-sur-Yvette, 91190, France. Tel.: +33 1 69 82 38 12; Fax: +33 1 69 82 36 95; E-mail: Leung@isv.cnrs-gif.fr
[4]Present address: Laboratório de Ecofisiologia Molecular, Instituto de Tecnologia Química e Biológica (ITQB), 2781-901 Oeiras, Portugal
[5]These authors contributed equally to this work

secondary transporters involved in ion and metabolite uptake. These proton pumps do not exist in animals, but they are structurally and functionally equivalent to the Na^+/K^+ P-type ATPases that establish electrochemical gradients across membranes to drive nutrient transport (Palmgren, 2001; Lefebvre *et al*, 2003).

The yeast genome encodes two H^+-ATPases, one of which (named PMA1) is absolutely essential for nutrient uptake and maintenance of intracellular pH, as its disruption is lethal (Serrano *et al*, 1986). In higher plants, H^+-ATPases are encoded by families of 9–12 gene members (Arango *et al*, 2003). Their functions in a global physiological context have been initially probed by using pharmacological agents that alter their activities. Notably, the use of the fungal toxin fusicoccin (FC), an activator of H^+-ATPases has provided initial clues on their roles in ion/nutrient transport, germination, cell expansion and stomatal opening (Marre, 1979). FC-treated tomato cells also led to acidification of the growth culture medium (Schaller and Oecking, 1999; Frick and Schaller, 2002), and in whole tomato plants, it was found to induce the accumulation of salicylic acid (SA), as well as the constitutive expression of certain pathogen-inducible genes. Conversely, H^+-ATPase inhibitors were found to alkalinize the cell culture medium and induce wound response genes in whole plants. These results have been interpreted to suggest a general role for H^+-ATPases in defense signaling (Schaller and Oecking, 1999).

Direct genetic evidence for these diverse roles of H^+-ATPases, however, is still scarce. Although their basic function is to use ATP hydrolysis to pump protons, visible phenotypes from a limited number of insertion mutants of *Arabidopsis* H^+-ATPase isoforms (named from *AHA1* to *AHA11*) hint at their complex roles in different developmental contexts. For example, *AHA10* is active primarily in endothelial cells in the developing seed integument, and the corresponding mutant is compromised in the production of the flavonoid proanthocyanidin, resulting in transparent testa. This mutant also accumulates small vacuoles, although how this phenotype is related to the disrupted H^+-ATPase is unknown (Baxter *et al*, 2005). Likewise, *aha3* insertion mutations cause fully penetrant male gametophyte lethality (Robertson *et al*, 2004). On the other hand, the physiological function of *AHA4* is more enigmatic, as the insertion mutation causes the production of truncated transcripts and the semi-dominant phenotype of increased sensitivity to high salt (Vitart *et al*, 2001). In transgenic tobacco, the co-suppression of the widely expressed *PMA4* also led to pleiotropic abnormalities related to nutrient transport (Zhao *et al*, 2000). Importantly, a significant number of stomata in these transgenic plants no longer responded to FC by opening. This phenotype indeed corroborates with electrophysiological studies indicating that FC activates H^+-ATPases, which drive plasma membrane hyperpolarization to condition

stomatal opening (Assmann and Wang, 2001; Roelfsema and Hedrich, 2005).

Stomata provide the major pathway of gas exchange. Among environmental signals, light (particularly blue content) is a potent physiological stimulus of stomatal opening, by activating plasma membrane H^+-ATPases (Kinoshita *et al*, 2001). The current model suggests that activation of the pump requires the phosphorylation of its penultimate threonine, and that this active conformation is stabilized by the binding of 14-3-3 proteins (Kinoshita and Shimazaki, 1999; Emi *et al*, 2001). Stomatal closure, in contrast, is stimulated by elevated CO_2 levels (above ambient level of ~ 350 ppm), transition from light to darkness and abscisic acid (ABA), a hormone synthesized in response to drought stress. All three signals cause alkalinization of the apoplastic space (Hedrich *et al*, 2001; Jia and Davis, 2007), which is correlated with the concomitant attenuation of the plasmalemma H^+-ATPase activity.

So far, the sequence of the molecular events leading from ABA perception to stomatal closure has been charted with the most experimental detail. Still, any specific contribution of H^+-ATPases to stomatal closure has been contentious, likely due to the current idea that these pumps are general endpoints of membrane transport pathways and a lack of appropriate mutants. The effect of ABA on the basal H^+-ATPase activity is not known in detail. However, ABA ($10 \mu M$ tested) inhibits ~ 60–65% of the blue light-induced H^+-ATPase activities in, respectively, guard cell protoplasts or intact guard cells from *Vicia faba* (Zhang *et al*, 2004) and *Arabidopsis* (Roelfsema *et al*, 1998). The underlying reason for the partial inhibition leaves unresolved the possible mechanisms. First, if ATPases were indeed general signaling endpoints, the partial inhibition would be indiscriminate or could even be indirectly caused by the non-physiological concentrations of applied ABA. At the other extreme, among the members in the proton pump family it could be that only some are susceptible to ABA inhibition because of their direct and specific implication in an ABA signaling pathway. Second, ABA activates the rapid- (R) and slow- (S)anion channels massively, and this has been proposed as the rate-limiting step to instigate as well as to sustain membrane depolarization necessary to drive K^+ efflux during stomatal closure (Schroeder and Keller, 1992; Schwartz *et al*, 1995; Ward *et al*, 1995; Roelfsema *et al*, 2004; Levchenko *et al*, 2005). In these models, the sustained activities of the anion channels have been assumed to be sufficient in magnitude to simply override those of the proton pumps. This impression has indeed been reinforced by recent proposals in which the inactivation of H^+-ATPase was considered to be irrelevant to stomatal closure (Levchenko *et al*, 2005).

We report here the identification of two dominant mutations (*D*) at the *open stomata 2* locus (Merlot *et al*, 2002) that abolish completely the guard cell's response to ABA, but importantly, only weakly to CO_2 and darkness. The *OST2* gene encodes the major H^+-ATPase previously named AHA1 (Harper *et al*, 1989), for which a physiological function had not been attributed. Both *ost2* mutations lead to constitutive activity of the pump and this has allowed us to evaluate critically the contribution of H^+-ATPases to stomatal closure. Our results strongly suggest that AHA1 is a principle target of inhibition by the ABA signal during drought response. A further implication is that in guard cells ABA operates

through a pathway that is, at least in part, distinct from those of CO_2 and darkness (Iba and Schroeder, 2006), even though all three signals promote stomatal closure, and this pathway distinction extends to the level of the proton pumps. The differential sensitivity of only certain H^+-ATPases (such as AHA1) to ABA could explain the incomplete nature of the inhibition by the hormone (Roelfsema *et al*, 1998; Zhang *et al*, 2004). Finally, since the *ost2* mutations cause constitutive and ABA-insensitive AHA1 activity, it is likely that in the wild type, ABA reverses the membrane potential by dynamically coordinating the inactivation of the proton pump, as well as the activation of anion channels.

Results

The ost2 mutations selectively impair stomatal response to ABA

The *Arabidopsis ost2-1D* mutant was previously isolated under progressive drought conditions, based on lower leaf temperature, as visualized by infrared imaging (Merlot *et al*, 2002). Further phenotypic characterization revealed that the mutant is prone to wilt even in well-watered growth conditions, shows stunted growth and reduced fertility (Figure 1A). Necrotic lesions, which are accentuated by increasing temperature and day length, appear on the rosette leaves of 1- to 2-week-old seedlings (see later). The leaf temperature of *ost2-1D* is on average $\sim 1^\circ C$ lower than that of wild type (L*er*) (Merlot *et al*, 2002). As shown in Figure 1B, this cooler temperature is correlated with a higher rate of transpirational water loss, as the fresh weight of the excised *ost2-1D* leaves decreased more rapidly over time relative to that of wild type leaves. At the cellular level, this mutant phenotype can be explained by the complete insensitivity of the guard cells to exogenous ABA (Merlot *et al*, 2002). The stomata of *ost2-1D* are about 1.5-fold more open relative to those of the wild type, and moreover, they do not close in response to even up to $100 \mu M$ ABA (Figure 1C). To define more precisely the nature of ABA signal interfered by *ost2-1D*, we tested stomatal closure in response to two other key signaling intermediates. Perception of ABA triggers the NADPH oxidase-mediated production of reactive oxygen species (H_2O_2), which then causes a rise in cytoplasmic Ca^{2+} (Pei *et al*, 2000; Kwak *et al*, 2003). H_2O_2 elicited a modest closure response in *ost2-1D*, while none was observed with Ca^{2+} (Figure 1D). Significantly, the *ost2-1D* stomata showed clear responsiveness to two other signals that provoke stomatal closure: transition from light to darkness and CO_2 (Figure 1E). A second mutant was isolated in the Col-0 accession from an independent thermal imaging screen that was based on the primary phenotype of larger stomatal aperture in darkness (Figure 1F, right panel; M Costa and B Genty, unpublished results). Like *ost2-1D*, rosette leaves of this second mutant also displayed necrosis. We have subsequently confirmed that this new mutation is allelic to *ost2-1D*, based on co-segregation with specific polymorphic DNA markers (Figure 2), and by DNA sequencing of the *OST2* gene. We named this second allele *ost2-2D*. Note that in contrast to *ost2-1D*, the basal stomatal aperture of *ost2-2D* is virtually identical to that of the wild type (Col-0) (Figure 1F, left panel). In spite of this, the pre-opened stomata of *ost2-2D* are still not responsive to applied ABA, even at high doses. The ability of the *ost2* mutants to respond to CO_2
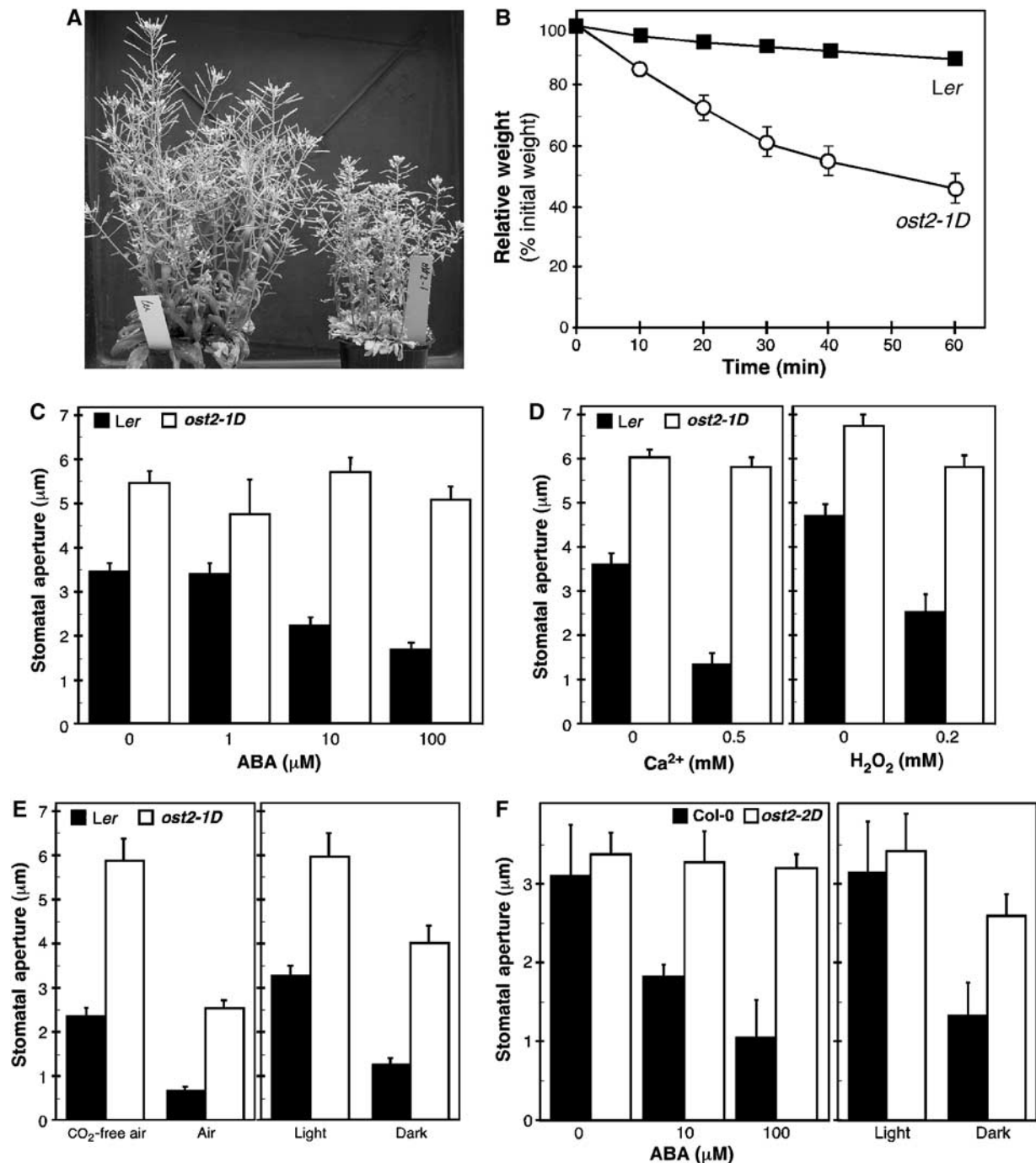
Figure 1 The *ost2* mutations inhibit ABA-induced stomatal closure. (**A**) *ost2-1D* is stunted in development and prone to wilt relative to the wild-type L*er*, even when well watered. (**B**) The kinetics of weight loss of detached leaves were compared between L*er* and *ost2-1D* (mean value ± s.d.; $n = 5$). (**C**) ABA-induced stomatal closure. Epidermal peels with stomata pre-opened by light were incubated for 3 h with the indicated concentrations of ABA. ABA at 100 μM induces stomatal closure by 52% in L*er* and 7% (*) in *ost2-1D*. (**D**) Ca^{2+}- and H_2O_2-induced stomatal closure. Epidermal peels with pre-opened stomata were incubated for 2 h with $CaCl_2$ or H_2O_2 at the indicated concentrations. (**E**) Stomatal opening in response to CO_2-free air was measured by using epidermal peels with pre-closed stomata incubated for 3 h in the dark with either normal or CO_2-depleted air. CO_2 (∼350 p.p.m.) inhibits stomatal opening by 72% in L*er* and by 57% in *ost2-1D*. To measure stomatal closure stimulated by light to darkness transition, epidermal peels with stomata pre-opened by light were incubated for 2.5 h in darkness. Darkness induces stomatal closure by 61% in L*er* and by 33% in *ost2-1D*. (**F**) ABA- and darkness-induced stomatal closure in the *ost2-2D* mutant and Col wild type. ABA at 100 μM induced stomatal closure by 66% in Col and by 5% (*) in *ost2-2D*. Darkness induced stomatal closure by 58% in Col and by 24% in *ost2-2D*. Each experiment was repeated four times. Data from one representative experiment are shown as the mean value ± s.e.m. ($n = 60$ stomata). The asterisk (*) indicates no statistical difference from 0 μM ABA ($P \leqslant 0.05$).

and darkness, but not to ABA, suggests that the corresponding gene product has a specific role in an ABA-dependent pathway controlling stomatal closure in response to drought (Figure 1E and F).

OST2 encodes a plasma membrane H^+-ATPase

The dominant mutation *ost2-1D* was mapped initially to a 125-kb region between the markers F19F24-*Ssp*I and F27F23-3 on chromosome 2 (Figure 2A). Despite repeated efforts,
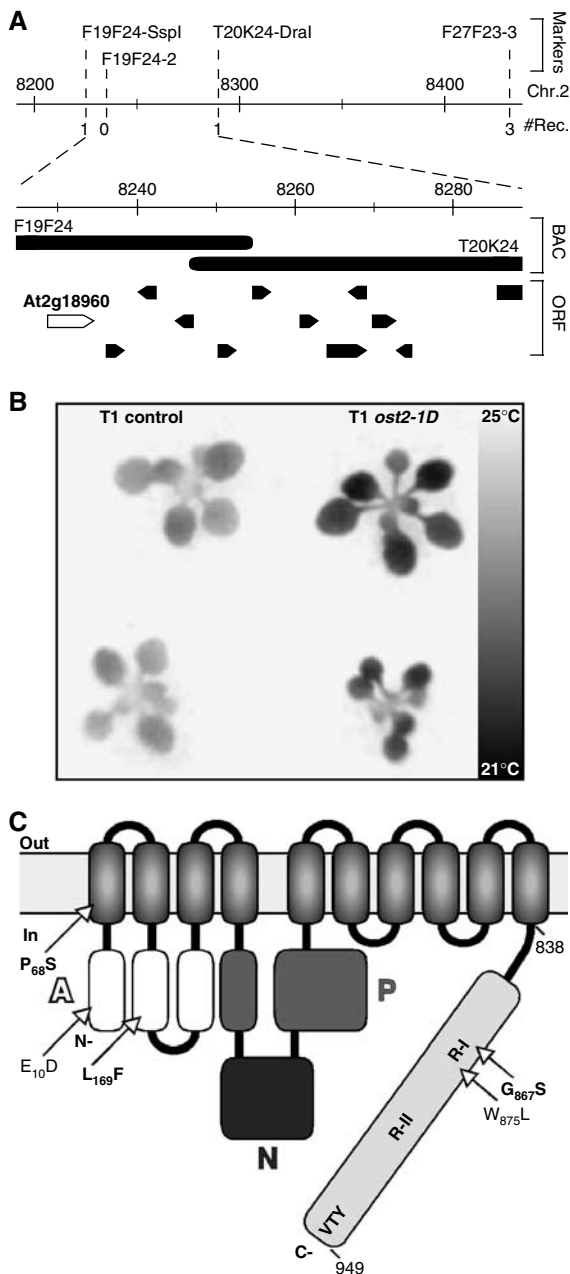
Figure 2 Identification of the *OST2* gene. (**A**) Genetic and molecular mapping of the *ost2-1D* mutation on chromosome 2. This region encompasses 12 open reading frames, including At2g18960 corresponding to the *OST2* gene. (**B**) Expression of the mutant At2g18960 gene in transgenic wild-type plant induces the *ost2-1D* phenotypes. Thermal imaging of plants transformed with either a genomic fragment cloned from the *ost2-1D* mutant comprising of At2g18960 and its promoter region (rosettes on right), or the truncated version of this genomic fragment lacking the promoter region and the N-terminal part of At2g18960 as control. (**C**) Schematic representation of AHA1 with the *ost2-1D* ($P_{68}S$) and *ost2-2D* alleles ($L_{169}F/G_{867}S$ in bold), or other mutations ($E_{10}D$ and $W_{875}L$) that rescue lethality of the yeast RS-72. A, N and P stand for actuator, nucleotide binding and phosphorylation domains, respectively.

recombination could not be detected in this interval in the F2 mapping populations generated by crosses to Col-0 as the parent. However, when WS was used as the parent instead of Col-0, the recombination limits demarcating *ost2-1D* were

reduced to 73 kb between F19F24-*Ssp*I and T20K24-*Dra*I, which encompass 12 open reading frames (ORFs). We combined sequencing and functional tests by introducing mutant *ost2-1D* genomic DNA covering this region into wild type *Arabidopsis*, to identify the gene. In particular, the complete sequencing of the four ORFs closest to F19F24-*Ssp*I (from At2g18960 to At2g19100) revealed that *OST2* most likely corresponded to At2g18960 (Figure 2A), annotated as the plasma membrane proton pump (H^+)-ATPase AHA1 (Harper *et al*, 1989). The gene would encode a protein of 949 amino acids, and the *ost2-1D* mutation predicts a non-conservative substitution of Pro_{68} to Ser ($P_{68}S$) in the first presumptive transmembrane segment (Figure 2C). Indeed, when a 9.9-kb *Nhe*I genomic fragment comprising of the *ost2-1D* mutant ORF and 4 kb of putative promoter sequences were introduced into wild-type *Arabidopsis*, the transgenic T1 plants (five independent lines) displayed lower foliar temperatures (Figure 2B) as well as necrotic lesions on rosette leaves (data not shown). The *ost2-2D* allele was found to harbor two missense mutations in the coding region of *AHA1* (Figure 2C): a C-to-T transition converting Leu_{169} to Phe ($L_{169}F$), and a G-to-A change converting Gly_{867} to Ser ($G_{867}S$). Also, as no other ORF outside of At2g18960 recapitulated the *ost2-1D* phenotypes in functional tests by plant transformation (data no shown), we conclude that *OST2* encodes the H^+-ATPase AHA1 (see Supplementary data).

The ost2 mutant genes efficiently rescue a yeast ATPase mutant

For clarity, we refer to the wild-type *OST2* by the original nomenclature of *AHA1*, and the mutant forms as *ost2*. We asked whether the dominance of the *ost2* mutations reflects a deregulation inherent in the properties of the pump itself, or its altered interaction with other regulators. Toward this, a functional assay based on yeast complementation was used. Previously, a mutant form of AHA1, with Trp (W)$_{875}$ (originally numbered W_{874}) replaced by Leu ($W_{875}L$), but not its wild-type counterpart, was shown to rescue the lethal growth defect of the yeast mutant RS-72 disrupted in its endogenous plasma membrane ATPase PMA1 (Cid *et al*, 1987; Baunsgaard *et al*, 1996) (Figure 3A). The superior efficacy of the mutated *AHA1* in this yeast complementation was interpreted to reflect a constitutive ATPase activity (Baunsgaard *et al*, 1996). Along this same line of argument, the mutation Pro_{72} to Ala ($P_{72}A$) in the tobacco ATPase PMA2 also efficiently rescued the yeast mutant (Morsomme *et al*, 1998). Protein alignments revealed that Pro_{72} of PMA2 is coincidental to Pro_{68} mutated in *ost2-1D*. In this latter case as well, *ost2-1D* but not *AHA1* complemented RS-72 (Figure 3A). Nearly identical results were also obtained with the *ost2-2D* allele, albeit its effectiveness was relatively less pronounced. To determine whether both mutations in *ost2-2D* were necessary for this complementation, we transformed RS-72 with the *OST2* gene carrying either the $G_{867}S$, or the other $L_{169}F$ amino-acid substitution. Yeast cells expressing the $G_{867}S$ mutation complemented to the same extent as the original *ost2-2D* allele, while no rescue was observed with the Leu_{169} substitution (Figure 3A). Therefore, it appears that the $G_{867}S$ in *ost2-2D* alone is responsible for the constitutive activity of AHA1, and by logical extension, probably the excessive transpiration phenotype as well.
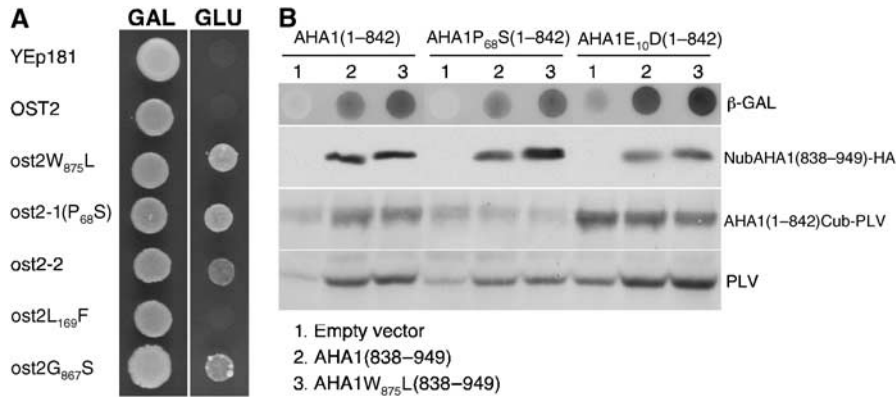
Figure 3 The *ost2-1D* and *ost2-2D* genes complement the yeast RS-72. (**A**) Complementation of the yeast mutant RS-72 in which the essential gene encoding the H$^+$-ATPase PMA1 was placed under the strict control of a galactose (GAL)-inducible promoter. The *ost2* genes with the mutations P$_{68}$S (*ost2-1D*) and G$_{867}$S (in *ost2-2D*), but not the wild-type *AHA1*, are able to complement the growth defect of RS-72. (**B**) Testing intramolecular interaction between the C-terminal regulatory domain and the remaining protein fragment of AHA1 using the yeast two-hybrid test based on split ubiquitin. Both the N-terminal moiety (aa 1–842) and the C-terminal regulatory domain (aa 838–949) were expressed as Cub-PLV and NubHA fusion protein, respectively. Interaction between the two parts of AHA1 causes cleavage release of the synthetic PLV transcription factor from Cub. PLV is then transported to the nucleus to activate the *LacZ* gene whose reporter expression is detectable as a blue color in the presence of X-gal. The expression levels of the different protein domains were compared by immunoblotting using either anti-HA or anti-VP16.

The current model on how the activity of plant H$^+$-ATPases is modulated is based in part on the intramolecular interaction of the protein. In its 'inhibited' state, the protein is thought to assume a highly folded conformation, with its C-terminal regulatory domain in contact with different cytoplasmic regions scattered throughout the rest of the protein (Palmgren, 2001; Lefebvre *et al*, 2003). In contrast, the 'activated' state of the protein is thought to be a more open structure, with its hinged C-terminal domain swinging away from the contact sites. Consistent with this is that deletion of the entire C-terminal domain leads to a constitutively activated ATPase in yeast (Palmgren and Christensen, 1993). One simple explanation for the presumed constitutive activity of the ost2 ATPase would be that the P$_{68}$S and G$_{867}$S substitutions obstruct intramolecular contacts between the C-terminal domain and the cytoplasmic sites, keeping the ATPase permanently in the more open, and therefore activated, conformation. Using the split ubiquitin system (Obrdlik *et al*, 2004), we first tested the model of intramolecular interaction proposed for ATPases, by co-transforming yeast with the C-terminal domain of AHA1 (AHA1$_{838-949}$ fused to Nub) and the rest of the protein (AHA1$_{1-842}$ fused to Cub-PLV). Indeed, transformants bearing both constructs expressed significantly stronger β-galactosidase reporter activity than those harboring the AHA1$_{1-842}$Cub-PLV moiety alone (Figure 3B). The increased β-galactosidase activity was also quantitatively proportional to the PLV released from the AHA1$_{1-842}$Cub-PLV protein as a second reporter for positive interaction (Figure 3B, bottom). Our results are thus in concordance with the proposed intramolecular interactions of the ATPase in its 'inhibited' state. Unexpectedly, however, the P$_{68}$S mutation did not abrogate its interaction with the C-terminal domain. Similarly, the mutations W$_{875}$L (Baunsgaard *et al*, 1996) and E$_{10}$D (coincidental to the tobacco PMA2 E$_{14}$D; Morsomme *et al*, 1998) that led to constitutive ATPase activity also did not noticeably affect interaction with the C-terminal domain. One possible explanation is that these mutations, while they deregulate the ATPase activity, may do so by another mechanism that is independent of the 'open' protein configuration predicted by the model. Alternatively, this supposed open configuration involves changes in the protein structure without a complete dissociation of the C-terminal domain from the rest of the protein.

Expression profile of OST2 in relation to cell size and metabolic activity

AHA1 has been reported to be expressed throughout plant development, and the transcript level seems to be refractory to most abiotic and biotic stimuli tested (http://www.Genesvestigator.ethz.ch/ and the e-FP browser at http://bbc.botany.utoronto.ca/). However, under our progressive drought conditions (Merlot *et al*, 2002), the *AHA1* transcript in leaves was marginally but consistently upregulated in both the wild type and in the mutant, as determined by DNA chip analysis using the CATMA version II array (Jammes *et al*, 2005) (slightly less than two-fold; combined data from three experimental repeats for each genotype; $P \leqslant 0.05$; data can be found at http://urgv.evry.inra.fr/cgi-bin/projects/CATdb/consult_project.pl?project_id = 15). The equal enhancement of the transcript in response to drought in both the *ost2-1D* mutant and the wild type indicates that its abundance is not subjected to negative feedback regulation.

Previous studies based on RNA blotting analysis and RT–PCR indicated that *AHA1* is expressed in roots and leaves, including guard cells (Harper *et al*, 1990; Ueno *et al*, 2005). To analyze its developmental expression profile in detail, we have generated transgenic plants expressing the reporter β-glucuronidase (GUS) gene under the control of the putative *AHA1* promoter (Figure 4). One of the most commonly attributed role to H$^+$-ATPases is in cell expansion due to acidification and loosening of the cell wall. However, in cells expressing *AHA1*, particularly in guard cells (Figure 4B), no significant difference in cell size between *ost2-1D* and the wild type was detected (data not shown). We note, furthermore, that the expression of *AHA1* is not detectable in the elongating radicle in the germinating seed (Figure 4F), as well as being excluded from the elongation zone of the root during
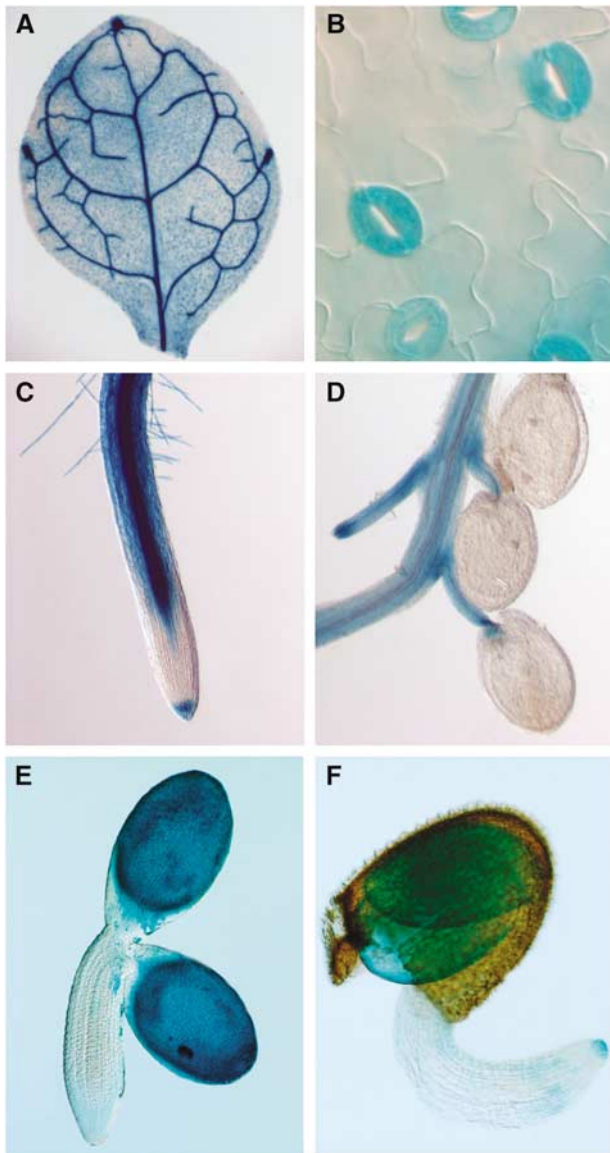
Figure 4 Expression profile of the *OST2* gene. Plants (Col) were transformed with the *pOST2::GUS* construct. GUS expression (blue) was detected in leaf veins (**A**), guard cells (**B**), primary root, except cells in the elongation zone (**C**), vascular tissues of young siliques (**D**), and during the late phase of embryo development (**E**) and at germination (**F**). No GUS activity was detected in mesophyll in any of the transgenic plants. Also, GUS activity was detected in trichomes and pollen, but tended to be variable among progeny even from a single transgenic line (data not shown).

seedling growth (Figure 4C). These results are similar to a previous report showing only weak immunological signals for a major H$^+$-ATPase isoform in the oat root meristem and the elongation zone (Parets-Soler *et al*, 1990). It also indicates that AHA1 does not play a general or prominent role in the control of cell expansion. However, strong promoter activity was detected in vascular tissues (leaves, roots and in the siliques) (Figure 4A, C and D), consistent with the known high solute transport activity of these cells.

The ost2-1D promotes SA-induced necrosis

As described earlier, the *ost2-1D* and the *ost2-2D* mutants developed spontaneous necrosis on leaves (Figure 5A). Dead cells, as revealed by staining with trypan blue (Koch and Slusarenko, 1990), are found frequently at the edges of leaves from *ost2-1D* but not those from the wild type. In addition, localized and microscopic-sized trypan blue stainings were observed near the veins where *AHA1* is strongly expressed (Figure 4A). As the leaf matures, these stained areas spread progressively, resulting in visible necrotic spots on the surface. These symptoms are similar to hypersensitive reaction triggered by SA, whose accumulation can be caused by the strong activation of plasma membrane H$^+$-ATPase activity (Schaller and Oecking, 1999). In accordance, the SA content in the rosettes of *ost2-1D* is about six times that found in the wild type (Figure 5B). The necrosis (but not the excessive transpiration; data not shown) can be suppressed by introducing the *NahG* gene encoding the SA hydroxylase, thus supporting a direct link of the symptoms to the elevated SA content (Figure 5C). This is confirmed further at the molecular level. *NahG* also suppressed the SA-responsive marker genes, *PATHOGENESIS RELATED PROTEIN1* (*PR1*, reduced about 10 000-fold) and *DEFENSIN* (*DEF*, about 10-fold) in the *ost2-1D* background (Figure 5D). Thus, all these diverse lines of indirect evidence are coherent with the data from yeast complementation that the *ost2-1D* mutation causes a constitutively activated ATPase.

The ost2-1D causes higher proton extrusion in plants

We sought to obtain direct evidence that the ost2 ATPase is in fact constitutively activated *in planta*. Compared to the wild type, the ost2 plasma membrane H$^+$-ATPase would be expected to extrude more protons into the apoplastic or extracellular space. Using epidermal preparations enriched in guard cells, obtained from the wild type kept in darkness, strongly enhanced acidification of the medium was detected by using a pH-sensitive microelectrode, when FC was added to stimulate the H$^+$-ATPases (Figure 6A). The guard cell-enriched epidermal preparations from *ost2-1D*, by contrast, acidified the medium even without FC (Figure 6A). We then compared the free-running potentials of their guard cell plasma membrane. In wild type (*Ler*), this ranged from -25 to -59 mV (mean $= -44.85 \pm 5.08$ mV; $n = 13$), and in *ost2-1D*, from -52 to -112 mV (mean $= -76,60 \pm 14.41$ mV; $n = 10$), indicating that the plasma membrane is more polarized in *ost2-1D* (Figure 6B). *AHA1* is also expressed in most parts of the root (Figure 4C). Seedlings transferred onto culture medium containing the pH-sensitive dye bromocresol purple cause it to turn yellow due to acidification (below pH 5.2). It is evident that the roots of the *ost2-1* acidify the medium more than those of the wild type (Figure 6C). These data provide direct support that the *ost2-1D* mutant allele causes constitutive AHA1 activity *in planta*.

Discussion

Light induces stomatal opening while ABA promotes closing. During the course of the day, the plant must continually adjust the conflicting needs for CO$_2$ uptake necessary for photosynthesis, while minimizing water loss through transpiration. Membrane transport governing stomatal opening had earlier been inferred by the use of FC and light (Assmann and Shimazaki, 1999; Kinoshita and Shimazaki, 1999, 2001). Both stimuli activate the H$^+$-ATPases to hyperpolarize the plasma membrane, which is coupled to potassium uptake
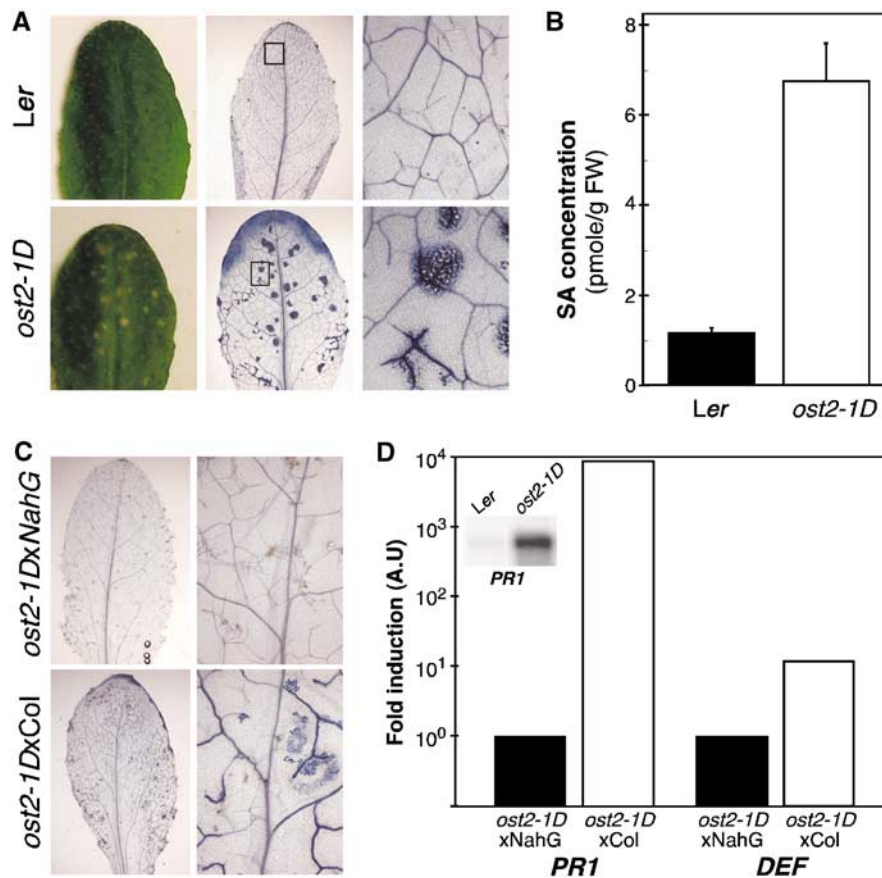
Figure 5 Hypersensitive response-like spontaneous necrosis in *ost2-1D* depends on SA signaling. (**A**) Dead cells are stained by trypan blue in Ler (top) and *ost2-1D* leaves (bottom). Dead cells in *ost2-1D* are at leaf edges and in localized area (middle) corresponding to the necrotic spots on the leaf (left). (**B**) Quantification of SA in Ler and *ost2-1D* leaves (10 rosettes from each genotype; two independent experiments). (**C**) Trypan blue staining of leaves of F1 plants from a cross of the *ost2-1D* dominant mutant with Col (bottom), or with Col plants expressing the SA hydroxylase encoded by *NahG* (top). (**D**) Comparison by quantitative RT–PCR of the transcript level of *Pathogenesis Related Protein1* gene (*PR1*, At2g14610) that is constitutively expressed in *ost2-1D* (northern blot in the inset), and the *DEFENSIN* gene *PDF1-2* (At5g44420) in F1 plants derived from *ost2-1D*xCol and *ost2-1D*xNahG. Their transcript levels were quantified by the $\Delta\Delta C\tau$ method (Livak and Schmittgen, 2001) and normalized with the constitutively expressed *EF1α* gene.

and the bowing of guard cells to open the stomatal pore. Apart from a number of P-type ATPases that transport Ca^{2+} or heavy metal (Axelsen and Palmgren, 2001), the H^+-ATPase is the only primary active transporter in the plasma membrane, making it probably the central component in driving stomatal opening.

In contrast, the role, if any, of these proton pumps in the signaling events leading to stomatal closing had been long debated. All current models concur on the massive activation of R- and S-anion channels by ABA as necessary and sufficient to depolarize the membrane potential leading to stomatal closing (Schroeder and Keller, 1992; Schwartz *et al*, 1995; Ward *et al*, 1995; Levchenko *et al*, 2005). Although the global H^+-ATPase activities are known to be diminished in the presence of exogenous ABA (Roelfsema *et al*, 1998; Zhang *et al*, 2004), the physiological significance of this has been ambiguous. The identification and characterization of the *ost2* mutations hence contribute to clarifying several points. First, these mutant guard cells show complete insensitivity to ABA, but they are still responsive to high CO_2 and darkness (Figure 1C–F). This strong ABA insensitivity is not caused by an indirect effect of the higher AHA1 activity impeding ABA uptake into the cell, since the protein kinase OST1 is still activated by exogenous ABA in the *ost2-1* mutant

(F Fenzi, unpublished data). AHA1 is therefore not a general endpoint of all signaling pathways impinging on membrane transport. Second, functional specialization among certain H^+-ATPases in ABA signaling could readily explain the partial inhibitory effect of the overall pump activities by the hormone. Third, the 'open stomata' phenotype caused by the constitutive *ost2* H^+-ATPase activity implies that the R- and S-anion channel currents are not sufficient to sustain plasma membrane depolarization to close stomata without curtailing the proton pump activity. The mechanisms that inactivate these pumps are currently unknown, but one that is phosphorylation based seems conceivable, as mutations in a pair of homologous protein phosphatases 2C (*abi1-1* and *abi2-1*) block ABA suppression of the global H^+-ATPase activities (Roelfsema *et al*, 1998).

Consistent with the hypothesis that the *ost2* mutations affect the regulation of the AHA1 activity is that the mutant genes, but not the wild type, complemented the growth defect of the yeast RS-72 (Figure 3A). Moreover, guard cells and roots from the mutant acidify the medium more readily that those from the wild type (Figure 6A and C). As a consequence of the increased proton extrusion, guard cell plasma membrane is hyperpolarized (Figure 6B). Also, certain pathogen-related genes are upregulated in *ost2-1D*. This upregulation is
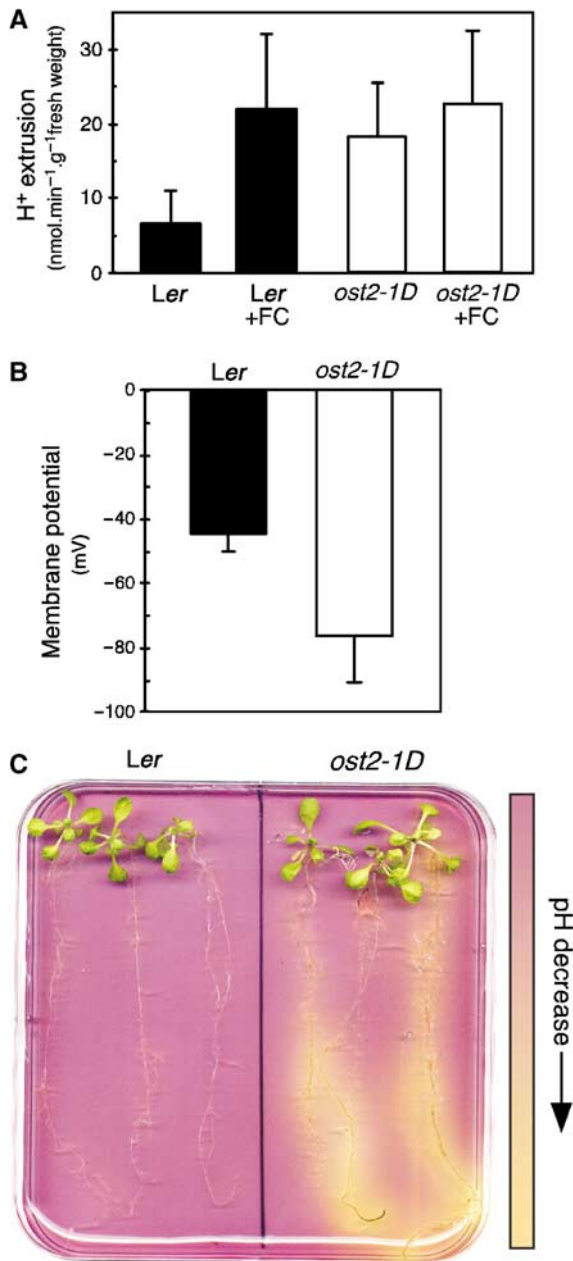
Figure 6 The *ost2-1D* mutation increases the activity of AHA1 *in planta*. (**A**) The rate of H^+ extrusion from stomatal-enriched cell fraction. Guard cells of wild type (L*er*) and *ost2-1D* were kept in darkness and incubated with or without FC and the pH of the external medium was continuously recorded to calculate the speed of H^+ extrusion (8–18 experiments ± s.e.m.). (**B**) Guard cell plasma membrane potential (V_m) was measured by dSEVC in both wild type (L*er*) and *ost2-1D*. Measured V_m ranged from –25 to –59 mV in L*er* (mean = -44.85 ± 5.08 mV; $n = 13$) and from –52 to –112 mV in *ost2-1D* (mean = -76.60 ± 14.41 mV; $n = 10$) (**C**) Visualization of medium acidification around the root system of 3-week-old plants using a colorimetric assay based on the pH-sensitive dye bromocresol purple at pH 6. This experiment was repeated four times with similar results.

due directly to an abnormally high content of SA because of its reversibility by *NahG* gene (Figure 5). These phenotypes are reminiscent of FC effects and entirely consistent with ost2 being a constitutively activated proton pump. Furthermore, results from our whole-genome RNA profiling experiments indicated that the most frequently encountered groups of upregulated genes in *ost2-1D* are those inducible by pathogens, SA and drought (see Supplementary data; complete files are available at http://urgv.evry.inra.fr/cgi-bin/projects/CATdb/consult_project.pl?project_id = 15). While it is known that FC triggers SA synthesis and subsequent pathogen-related responses, our data support that among the FC targets, at least an H^+-ATPase is involved. The underlying mechanism linking an activated H^+-ATPase to higher SA content is not known. However, the parallel between FC treatment and the mutational consequences is not complete. There is no correlation between the tissues in which *ost2-1D* is expressed and significant cell enlargement, nor noticeably enhanced general pathogen resistance, at least to *Pseudomonas syringae* (AvrRpm1) and *Pithyum phytophthora* that we have tested (data not shown). FC is now known to have a broader spectrum of physiological effects than previously expected. It targets different 14-3-3 isoforms (Wurtele *et al*, 2003), which in turn have multiple or even opposing effects on ion transport, by their binding to diverse cellular components in addition to H^+-ATPases (Bunney *et al*, 2003; van den Wijngaard *et al*, 2005).

Although both *ost2-1D* and *ost2-2D* mutations impair ABA response, nonetheless, they foster distinct stomatal phenotypes under normal experimental growth conditions. The basal stomatal aperture of *ost2-2D* is hardly distinguishable from that of the wild type, while that of *ost2-1D* is always more open (Figure 1C and F). The P_{68} mutated in *ost2-1D* coincides with P_{72} of the tobacco PMA2, whose mutation to serine was also shown to cause higher ATPase activity based on yeast complementation (Morsomme *et al*, 1998). This conserved proline is predicted to locate in the first transmembrane segment (Figure 2C). The *ost2-2D* allele contains two mutations, $L_{169}F$ and $G_{867}S$ (Figure 2C). While we cannot formally rule out that both mutations are necessary for the ABA-insensitive stomata phenotype, the latter mutation alone clearly rescued the yeast mutant as efficiently as the original *ost2-2D* allele, while the $L_{169}F$ did not (Figure 4). The amino acid G_{867} is conserved in the *Arabidopsis* proton pump AHA2, and it is localized in the so-called RI domain in the auto-inhibitory C-terminus (Figure 2C). Consistent with our results, it has been reported that the $G_{867}A$ mutation introduced in *aha2* also complemented more efficiently the yeast RS-72 than the wild-type *AHA2* (Axelsen and Palmgren, 2001). Taking these findings together, mutations in these conserved residues (P_{68} and G_{867} in AHA1 and equivalent amino acids in other H^+-ATPases) appear to render the proton pump constitutively activated.

The $P_{72}A$ mutation in the tobacco PMA2 increased its IC_{50} (50% maximum inhibitory concentration) to vanadate, an inhibitor of H^+-ATPase, from 11 to 80 μM, while no such change was observed for another mutation $W_{833}L$ in the RI domain (Morsomme *et al*, 1998). By analogy to the above, the enhancement of the AHA1 activity by the two *ost2* mutations could also be due to the disruption of distinct regulatory mechanisms. We note that the *ost2-1D* mutant exhibits constitutively larger stomatal opening. This phenotype may reflect that the corresponding protein is deregulated not only in the activation mechanisms of the pump but also its basal catalytic activity. In contrast, the basal stomatal aperture of *ost2-2D* is similar to that of the wild type, but the mutant guard cells are clearly refractory to ABA, while retaining partial sensitivities to other stimuli. Thus, the

mutant ost2-2D protein may not be more active under normal conditions, but it is altered in its mode of suppression by ABA during stress. This might be correlated with the fact that the mutation $G_{867}S$ maps to the regulatory domain.

It has been proposed that the higher activities of the plant mutant ATPases in yeast might be caused by weakened interaction between the autoinhibitory C-terminus and the rest of the protein (Palmgren, 2001). In support of this model, the mutant proteins are more accessible to trypsin digestion than the wild-type forms (Morsomme *et al*, 1998). For AHA1, we could show interaction between the C-terminus and the rest of the protein, consistent with intramolecular interactions in the 'off' state (Figure 4B). However, none of the mutations tested ($P_{68}S$, $W_{875}L$ in the RI domain and $E_{10}D$ in the N-terminus) abolished the 'intramolecular' interaction. This is a rather surprising observation in view of the proposed activation model based on trypsin accessibility, which suggests release of the C-terminal regulatory domain from the rest of the protein as the H^+-ATPase passes from 'off' to an active state. As a further analogy, the P-type sarcoplasmic reticulum Ca^{2+}-ATPase, whose catalytic domain is structurally similar to that of the H^+-ATPase, also undergoes pronounced changes during the catalytic process, as shown by enhanced trypsin accessibility to the catalytic core (Danko *et al*, 2001; Toyoshima and Nomura, 2002). Our results advance rather another possibility that structural reorganization of AHA1 during activation may not lead to complete dissociation of the regulatory C-terminal domain from the rest of the protein. There are probably still many possible types of regulations that govern the activity of H^+-ATPases (Arango *et al*, 2003), for which the precise mechanisms impaired by the different *ost2* mutations will need to be further explored. For example, these mutations may have altered the inherent propensity of the pumps to form hexamer, which is the activated form of the H^+-ATPases (Kanczewska *et al*, 2005), or accessibility to kinases and phosphatases as new phosphorylation sites on AHA1, in addition to the penultimate phospho-threonine involved in H^+-ATPase activation have been recently reported (Nuhse *et al*, 2003).

The expression of all 11 H^+-ATPase isogenes can be detected in *Arabidopsis* guard cell protoplasts, with *AHA1*, *AHA2* and *AHA5* being predominant (Ueno *et al*, 2005). Whether this is also the case in intact guard cells and in the whole-plant context is currently unknown. T-DNA insertion mutations have been described for *AHA3* and *AHA10* but no major visible stomatal defect has been reported (Robertson *et al*, 2004; Baxter *et al*, 2005). Also to our knowledge, no other forward genetic screen has revealed a similar role for the remaining ATPases in *Arabidopsis*. T-DNA insertions in the *AHA1* locus exist (Young *et al*, 2001; Arango *et al*, 2003), but failed to reveal its connection with ABA signaling, suggesting that it may be cloaked by redundant functions with other proton pumps (for example, AHA2 and AHA5). On the other hand, the lack of dominant mutations so far at either *AHA2* or *AHA5* could mean that these other major pumps may have different enzymatic properties (k_m, V_{max} and pH sensitivity) (Arango *et al*, 2003), whose mutations may not manifest into readily detectable stomatal phenotypes, under our experimental conditions. Evidence from the literature indicates that closely related H^+-ATPase isoforms could be distinguished by their different affinities for ATP or

vanadate (Villalba *et al*, 1992; Palmgren and Christensen, 1994) and pH sensitivities (Luo *et al*, 1999). Because the C-terminal autoinhibitory domains among the plant H^+-ATPases are divergent in sequences, they may also impose different modes of regulation, dictated by their affinity to different parts of the protein. The identification of the *ost2* mutants reinforces the idea that plant H^+-ATPases have intrinsic specificity, beyond differences in tissue expression that dedicate them to specific physiological functions in cells.

High atmospheric CO_2 also promotes stomatal closure, but current evidence suggests that this engages a signaling pathway different from that of ABA (Vavasseur and Raghavendra, 2004; Iba and Schroeder, 2006). Genetic screens based on infrared imaging for mutations that disrupt stomatal opening in response to low atmospheric CO_2 have identified two alleles at the locus *HIGH LEAF TEMPERATURE* (*HT1*) (Hashimoto *et al*, 2006). These allelic mutants, while indifferent to the atmospheric CO_2 levels, still responded partially to blue light and FC. More importantly, the stomata of *ht1*, like those of the wild type, closed when exposed to ABA and to darkness. ABA, CO_2 and light/dark transition may therefore employ distinct signaling pathways in the control of stomatal movements. The pathway demarcation clearly extends to the level of the H^+-ATPase isoforms, and our results here show that AHA1 is one of the key determinants that affect stomatal closure, in response to drought, via an ABA-directed pathway. A more complete understanding of the mechanisms that inactivate this H^+-ATPase will further highlight important elements of the drought stress signaling pathway, as well as provide new prospects for the improvement of drought hardiness in plants.

Materials and methods

Mutant screens and stomatal aperture assays
Mutant screens based on infrared thermography that identified *ost2-1D* (L*er*) have been described (Merlot *et al*, 2002). The *ost2-2D* allele (Col-0) was isolated using infrared imaging, for mutants with incompletely closed stomata in response to a transition from light to darkness (M Costa and B Genty, unpublished data). Stomatal responses to ABA, H_2O_2, Ca^{2+}, CO_2 and light to darkness transition were tested as described (Mustilli *et al*, 2002; Supplementary data), using leaves from 4- to 5-week-old plants. Results were from three independent sets of experiments performed by two different individuals.

Phytohormone analyses
Cellular content of SA was analyzed as described, using multiplex gas chromatography-tandem mass spectrometry (Müller *et al*, 2002). $[^2H]_4$-SA was included in the leaf samples as an internal standard, during extraction.

Tissue-specific activity of the OST2 promoter
The presumptive promoter of *OST2*, 2.47 kb upstream of the ATG start codon, was amplified from L*er* genomic DNA using specific oligonucleotides (see Supplementary data). The amplified DNA was cloned into *Eco*RI and *Nco*I sites of the T-DNA vector pCambia1381Z (www.Cambia.org). Five independent transgenic lines were analyzed by GUS histochemical staining.

Complementation of yeast mutant RS-72 with different ost2 alleles
Point mutations corresponding to the *ost2* alleles were introduced into the *AHA1* cDNA BX320549 by PCR, using the high-fidelity *Taq* polymerase Phusion (Finnezyme) and mutagenic primers (see Supplementary data for the list of primers), except for the mutation $W_{875}L$, which was obtained from the clone pMP353 (Baunsgaard *et al*, 1996). The mutated *aha1* genes were cloned as

*Bam*HI/*Bgl*II fragments into the *Bam*HI site of Yep181HE (Lowe *et al*, 2004), and confirmed by sequencing. These constructs were introduced into the yeast mutant RS-72 by lithium–polyethylene glycol treatment and transformants were selected on SC-UL medium containing galactose. To test the ability of the different *ost2D* alleles to complement RS-72, transformants growing on SC-UL galactose were transferred to SC-UL glucose medium, to inhibit expression of the endogenous *PMA1* gene (Cid *et al*, 1987). RS-72 transformed with pMP353 was used as positive control (Baunsgaard *et al*, 1996).

Protein interaction assays using the split ubiquitin system

Yeast two-hybrid experiments based on split ubiquitin were conducted as essentially described (Obrdlik *et al*, 2004). The wild-type and corresponding mutant N-terminal domains (aa 1–842) spanning the 10 transmembrane segments of AHA1 were amplified by PCR, using the Phusion polymerase, with primers MetAHA1CgateB1 and MetAHA1CgateB2 (Supplementary data), and cloned into metXCubgate vector by recombination in yeast. The wild-type and corresponding mutant C-terminal tail of AHA1 (aa 838–949) were amplified with primers pAHA1Ngate3HAB1 and pAHA1Ngate3HAB2 (Supplementary data) and cloned in pNubXgate3HA vectors as described above. pCub (C-terminus of ubiquitin) and pNub (N-terminus part) constructs were transformed, respectively, in the yeast strains AP4 and AP5. The different AHA1 domains were made to interact by mating these yeast strains. The expression of recombinant proteins was analyzed by immunoblotting using antibodies directed against the epitopes HA (3F10, Roche) and VP16 (7545, Santa Cruz).

H⁺ extrusion and membrane potential measurements from guard cell and root acidification assays

Epidermal strips enriched in guard cells were ultrasonicated for 3 s to remove pavement and mesophyll cells, as described (Kinoshita

and Shimazaki, 2001). The pH of the medium was measured according to the conditions specified in the Supplementary data. Free-running membrane potential (V_m) of *Arabidopsis* guard cells from open stomata was measured by the discontinuous single-electrode voltage-clamp (dSEVC) technique (Forestier *et al* 1998), using a solution containing 5 mM KCl, 5 mM potassium citrate, 100 μM CaCl$_2$, 1 mM MgCl$_2$ as bathing solution (Marten *et al*, 2007). For root acidification assays, roots from 3-week-old plants were spread on a nutrient agar medium containing 0.003% (w/v) bromocresol purple (pH 6.0), and the change in acidity of the medium was visualized according to conditions provided in the Supplementary data.

Supplementary data

Supplementary data are available at *The EMBO Journal* Online (http://www.embojournal.org).

References

Arango M, Gevaudant F, Oufattole M, Boutry M (2003) The plasma membrane proton ATPase: the significance of gene subfamilies. *Planta* **216:** 355–365

Assmann SM, Shimazaki K-i (1999) The multisensory guard cell. Stomatal responses to blue light and abscisic acid. *Plant Physiol* **119:** 809–815

Assmann SM, Wang X-Q (2001) From milliseconds to millions of years: guard cells and environmental responses. *Curr Opin in Plant Biol* **4:** 421–428

Axelsen KB, Palmgren MG (2001) Inventory of the superfamily of P-type ion pumps in *Arabidopsis*. *Plant Physiol* **126:** 696–706

Baunsgaard L, Venema K, Axelsen KB, Villalba JM, Welling A, Wollenweber B, Palmgren MG (1996) Modified plant plasma membrane H⁺-ATPase with improved transport coupling efficiency identified by mutant selection in yeast. *Plant J* **10:** 451–458

Baxter IR, Young JC, Armstrong G, Foster N, Bogenschutz N, Cordova T, Peer WA, Hazen SP, Murphy AS, Harper JF (2005) A plasma membrane H⁺-ATPase is required for the formation of proanthocyanidins in the seed coat endothelium of *Arabidopsis thaliana*. *Proc Natl Acad Sci USA* **102:** 2649–2654

Bunney TD, De Boer AH, Levin M (2003) Fusicoccin signaling reveals 14-3-3 protein function as a novel step in left–right patterning during amphibian embryogenesis. *Development* **130:** 4847–4858

Cid A, Perona R, Serrano R (1987) Replacement of the promoter of the yeast plasma membrane ATPase gene by a galactose-dependent promoter and its physiological consequences. *Curr Genet* **12:** 105–110

Danko S, Yamasaki K, Daiho T, Suzuki H, Toyoshima C (2001) Organization of cytoplasmic domains of sarcoplasmic reticulum Ca²⁺-ATPase in E(1)P and E(1)ATP states: a limited proteolysis study. *FEBS Lett* **505:** 129–135

Emi T, Kinoshita T, Shimazaki K (2001) Specific binding of vf14-3-3a isoform to the plasma membrane H⁺-ATPase in response to blue light and fusicoccin in guard cells of broad bean. *Plant Physiol* **125:** 1115–1125

Forestier C, Bouteau F, Leonhardt N, Vavasseur A (1998) Pharmacological properties of slow anion currents in intact guard cells of *Arabidopsis*. Application of the discontinuous single-electrode voltage-clamp to different species. *Pflügers Arch Eur J Physiol* **436:** 920–927

Frick UB, Schaller A (2002) cDNA microarray analysis of fusicoccin-induced changes in gene expression in tomato plants. *Planta* **216:** 83–94

Harper JF, Manney L, DeWitt ND, Yoo MH, Sussman MR (1990) The *Arabidopsis thaliana* plasma membrane H⁺-ATPase multigene family. Genomic sequence and expression of a third isoform. *J Biol Chem* **265:** 13601–13608

Harper JF, Surowy TK, Sussmann MR (1989) Molecular cloning and sequence of cDNA encoding the plasma membrane proton pump (H⁺-ATPase) of *Arabidopsis thaliana*. *Proc Natl Acad Sci USA* **86:** 1234–1238

Hashimoto M, Negi J, Young J, Israelsson M, Schroeder JI, Iba K (2006) *Arabidopsis* HT1 kinase controls stomatal movements in response to CO$_2$. *Nat Cell Biol* **8:** 391–397

Hedrich R, Neimanis S, Savchenko G, Felle HH, Kaiser WM, Heber U (2001) Changes in apoplastic pH and membrane potential in leaves in relation to stomatal responses to CO$_2$, malate, abscisic acid or interruption of water supply. *Planta* **213:** 594–601

Iba K, Schroeder JI (2006) Guard cell ABA and CO$_2$ signaling network updates and Ca²⁺ sensor priming hypothesis. *Curr Opin in Plant Biol* **9:** 654–663

Jammes F, Lecomte P, de Almeida-Engler J, Bitton F, Martin-Magniette M-L, Renou JP, Abad P, Favery B (2005) Genome-wide expression profiling of the host response to root-knot nematode infection in *Arabidopsis*. *Plant J* **44:** 447–458

Jia W, Davis WJ (2007) Modification of leaf apoplasitc pH in relation to stomatal sensitivity to root-sourced ABA signals. *Plant Physiol* **143:** 68–77

Kanczewska J, Marco S, Vandermeeren C, Maudoux O, Rigaud J-L, Boutry M (2005) Activation of the plant plasma membrane H⁺-ATPase by phosphorylation and binding of 14-3-3 proteins converts a dimer into a hexamer. *Proc Natl Acad Sci USA* **102:** 11675–11680

Kinoshita T, Doi M, Suetsugu N, Kagawa T, Wada M, Shimazaki K (2001) phot1 and phot2 mediate blue light regulation of stomatal opening. *Nature* **414:** 656–660

Kinoshita T, Shimazaki K (2001) Analysis of the phosphorylation level in guard-cell plasma membrane H⁺-ATPase in response to fusicoccin. *Plant Cell Physiol* **42:** 424–432

Kinoshita T, Shimazaki K-i (1999) Blue light activates the plasma membrane H$^+$-ATPase by phosphorylation of the C-terminus in stomatal guard cells. *EMBO J* **18:** 5548–5558

Koch E, Slusarenko A (1990) *Arabidopsis* is susceptible to infection by a downy mildew fungus. *Plant Cell* **2:** 437–445

Kwak JM, Mori IC, Pei ZM, Leonhardt N, Torres MA, Dangl JL, Bloom RE, Bodde S, Jones JD, Schroeder JI (2003) NADPH oxidase AtrbohD and AtbohF genes function in ROS-dependent ABA signaling in *Arabidopsis*. *EMBO J* **22:** 2623–2633

Lefebvre B, Boutry M, Morsomme P (2003) The yeast and plant plasma membrane H$^+$ pump ATPase: divergent regulation for the same function. *Prog in Nucl Acid Res* **74:** 203–237

Levchenko V, Konrad KR, Dietrich P, Roelfsema MR, Hedrich R (2005) Cytosolic abscisic acid activates guard cell anion channels without preceding Ca^{2+} signals. *Proc Natl Acad Sci USA* **102:** 4203–4208

Livak KJ, Schmittgen TD (2001) Analysis of gene expression data using real-time quantitative PCR and the $2^{-\Delta\Delta C}\tau$ method. *Methods* **25:** 402–408

Lowe J, Vieyra A, Catty P, Guillain F, Mintz E, Cuillel M (2004) A mutational study in the transmembrane domain of Ccc2p, the yeast Cu^{2+}-ATPase, shows different roles for each Cys–Pro–Cys cysteine. *J Biol Chem* **279:** 25986–25994

Luo H, Morsomme P, Boutry M (1999) The two major types of plant plasma membrane H$^+$-ATPases show different enzymatic properties and confer differential pH sensitivity of yeast growth. *Plant Physiol* **119:** 627–634

Marre E (1979) Fusicoccin: a tool in plant physiology. *Annu Rev Plant Physiol* **30:** 273–288

Marten H, Konrad KR, Dietrich P, Roelfsema MRG, Hedrich R (2007) Ca^{2+}-dependent and -independent abscisic acid activation of plasma membrane anion channels in guard cells of *Nicotiana tabacum*. *Plant Physiol* **143:** 28–37

Merlot S, Mustilli A-C, Genty B, North H, Lefebvre V, Sotta B, Vavasseur A, Giraudat J (2002) Use of infrared thermal imaging to isolate *Arabidopsis* mutants defective in stomatal regulation. *Plant J* **30:** 601–609

Morsomme P, Dambly S, Maudoux O, Boutry M (1998) Single point mutations distributed in 10 soluble and membrane regions of the *Nicotiana plumbaginifolia* plasma membrane PMA2 H$^+$-ATPase activate the enzyme and modify the structure of the C-terminal region. *J Biol Chem* **273:** 34837–34842

Müller A, Düchting P, Weiler EW (2002) A mulitplex GC-MS/MS technique for the sensitive and quantitative single-run analysis of acidic phytohormones and related compounds, and its application to *Arabidopsis thaliana*. *Planta* **216:** 44–56

Mustilli A-C, Merlot S, Vavasseur A, Fenzi F, Giraudat J (2002) *Arabidopsis* OST1 protein kinase mediates the regulation of stomatal aperture by abscisic acid and acts upstream of reactive oxygen species production. *Plant Cell* **14:** 3089–3099

Nuhse TS, Stensballe A, Jensen ON, Peck SC (2003) Large-scale analysis of *in vivo* phosphorylated membrane proteins by immobilized metal ion affinity chromatography and mass spectrometry. *Mol Cell Proteomics* **2:** 1234–1243

Obrdlik P, El-Bakkoury M, Hamacher T, Cappellaro C, Vilarino C, Fleischer C, Ellerbrok H, Kamuzinzi R, Ledent V, Blaudez D, Sanders D, Revuelta JL, Boles E, Andre B, Frommer WB (2004) K$^+$ channel interactions detected by a genetic system optimized for systematic studies of membrane protein interactions. *Proc Natl Acad Sci USA* **101:** 12242–12247

Palmgren MG (2001) Plant plasma membrane H$^+$-ATPases: power-houses for nutrient uptake. *Annu Rev Plant Physiol Plant Mol Biol* **52:** 817–845

Palmgren MG, Christensen G (1993) Complementation *in situ* of the yeast plasma membrane H$^+$-ATPase gene from a heterologous speices. *FEBS Lett* **317:** 216–222

Palmgren MG, Christensen G (1994) Functional comparison between plant plasma membrane H$^+$-ATPase isoforms expressed in yeast. *J Biol Chem* **269:** 3027–3033

Parets-Soler A, Pardo JM, Serrano R (1990) Immunocytolocalization of plasma membrane H$^+$-ATPase. *Plant Physiol* **93:** 1654–1658

Pei Z-M, Murata Y, Benning G, Thomine S, Klüsener B, Allen GJ, Grill E, Schroeder JI (2000) Calcium channels activated by hydrogen peroxide mediate abscisic acid signalling in guard cells. *Nature* **406:** 731–734

Robertson WR, Clark K, Young JC, Sussmann MR (2004) An *Arabidopsis thaliana* plasma membrane proton pump is essential for pollen development. *Genetics* **168:** 1677–1687

Roelfsema MR, Levchenko V, Hedrich R (2004) ABA depolarizes guard cells in intact plants, through a transient activation of R- and S-type anion channels. *Plant J* **37:** 578–588

Roelfsema MRG, Hedrich R (2005) In the light of stomatal opening: new insights into 'the Watergate'. *New Phytologist* **165:** 665–691

Roelfsema MRG, Staal M, Prins HBA (1998) Blue light-induced apoplastic acidification of *Arabidopsis thaliana* guard cells: inhibition by ABA is mediated through protein phosphatases. *Physiol Plant* **103:** 466–474

Schaller A, Oecking C (1999) Modulation of plasma membrane H$^+$-ATPase activity differentially activates wound and pathogen defense responses in tomato plants. *Plant Cell* **11:** 263–272

Schroeder J, Keller BU (1992) Two types of anion channel currents in guard cells with distinct voltage regulation. *Proc Natl Acad Sci USA* **89:** 5025–5029

Schwartz A, Ilan N, Schwarz M, Scheaffer J, Assmann SM, Schroeder JI (1995) Anion-channel blockers inhibit S-type channels and abscisic acid responses in guard cells. *Plant Physiol* **109:** 651–658

Serrano R, Kielland-Brandt MC, Fink GR (1986) Yeast plasma membrane ATPase is essential for growth and has homology with (Na$^+$+K$^+$), K$^+$- and Ca^{2+}-ATPases. *Nature* **319:** 689–693

Toyoshima C, Nomura H (2002) Structural changes in the calcium pump accompanying the dissociation of calcium. *Nature* **418:** 605–611

Ueno K, Kinoshita T, Inoue S-i, Emi T, Shimazaki K-i (2005) Biochemical characterization of plasma membrane H$^+$-ATPase activation in guard cell protoplasts of *Arabidopsis thaliana* in response to blue light. *Plant Cell Physiol* **46:** 955–963

van den Wijngaard PWJ, Sinnige MP, Boobeek I, Reumer A, Schoonheim PJ, Mol JNM, Wang M, De Boer AH (2005) Abscisic acid and 14-3-3 proteins control K$^+$ channel activity in barley embryonic root. *Plant J* **41:** 43–55

Vavasseur A, Raghavendra AS (2004) Guard cell metabolism and CO$_2$ sensing. *New Phytologist* **165:** 665–682

Villalba JM, Palmgren MG, Berberian GE, Ferguson C, Serrano R (1992) Functional expresson of plant plasma membrane H$^+$-ATPase in yeast endoplasmic reticulum. *J Biol Chem* **267:** 12341–12349

Vitart V, Baxter I, Doerner P, Harper JF (2001) Evidence for a role in growth and salt resistance of a plasma membrane H$^+$-ATPase in the root endodermis. *Plant J* **27:** 191–201

Ward JM, Pei Z-M, Schroeder JI (1995) Roles of ion channels in initiation of signal transduction in higher plants. *Plant Cell* **7:** 833–844

Wurtele M, Jelich-Ottmann C, Wittinghofer A, Oecking C (2003) Structural view of a fungal toxin acting on a 14-3-3 regulatory complex. *EMBO J* **22:** 987–994

Young JC, Krysan PJ, Sussman MR (2001) Efficient screening of *Arabidopsis* T-DNA insertion lines using degenerate primers. *Plant Physiol* **125:** 513–518

Zhang X, Wang H, Takemiya A, Song C-P, Kinoshita T, Shimazaki K-i (2004) Inhibition of blue light-dependent H$^+$ pumping by abscisic acid through hydrogen peroxide-induced dephosphorylation of the plasma membrane H$^+$-ATPase in guard cell protoplasts. *Plant Physiol* **136:** 4150–4158

Zhao R, Dielen V, Kinet J-M, Boutry M (2000) Cosuppression of a plasma membrane H$^+$-ATPase isoform impairs sucrose translocation, stomatal opening, plant growth, and male fertility. *Plant Cell* **12:** 535–546